Journal of Bridge Engineering. Submitted March 10, 2011; accepted September 14, 2011;
posted ahead of print September 16, 2011. doi:10.1061/(ASCE)BE.1943-5592.0000308

Retracted: Effective Flange Width for Honeycomb FRP Sandwich Bridge Deck-on-Steel Girder System with a Mechanical Shear Connector considering Degrees of Composite Action

An Chen[1], Julio F. Davalos[2]
Adam L. Justice[3], Gregory K. Michaelson[3], and Nagavardhana Perisetty[3]

Abstract

Effective flange width is used in bridge engineering to reduce a 3-D structure to a 2-D beam analysis. AASHTO Specifications provide provisions solely for effective flange width for concrete decks on steel girders with full-composite action. In recent years, FRP decks have been increasingly used because of their many advantages. An FRP deck-on-steel girder system exhibits either full or partial composite action, depending on the shear connection used to attach the deck to supporting girders. Since no design guidelines are available, the bridge system is often considered as non-composite, and therefore, the bridge is usually over-designed. This paper systematically evaluates effective flange width for honeycomb FRP sandwich deck-on-steel girder bridge system, accounting for either full or partial composite action, to propose a modified AASHTO equation to calculate the effective flange width. In this paper, a Finite Element (FE) model is first developed to predict effective flange width for FRP deck-on-steel girder system with partial composite action based on a proper definition of the effective flange width, which is then verified by testing results of a T-beam section. The FE model is then used to carry out a parametric study by varying the degree of composite action and stiffness of the bridge deck. Based on the results from the parametric study, a modified AASHTO equation is proposed to

[1] Research Assistant Professor, Department of Civil and Environmental Engineering, West Virginia University, Morgantown, WV 26506-6103. E-mail: an.chen@mail.wvu.edu (corresponding author)
[2] Benedum Distinguished Teaching Professor, Department of Civil and Environmental Engineering, West Virginia University.
[3] Graduate Research Assistants, Department of Civil and Environmental Engineering, West Virginia University (They contributed equally to this paper).

Journal of Bridge Engineering. Submitted March 10, 2011; accepted September 14, 2011;
posted ahead of print September 16, 2011. doi:10.1061/(ASCE)BE.1943-5592.0000308

calculate the effective flange width. Finally, an example is provided to illustrate the use of the proposed equation. It is concluded that the bridge stiffness and strength can be significantly increased by considering the proper contribution of the FRP deck, which is in contrast to the general impression that, because of the low equivalent modulus of the FRP deck, the contribution of the deck to the bridge system may be neglected, even for full-composite action.

Keywords: Effective Flange Width, Partial Composite Action, FRP, Finite Element Modeling, Parametric Study, Design Guideline.

Introduction

In bridge engineering, a deck-and-girder system acting compositely is usually analyzed using line girder analysis, in which a T-beam section is considered for computational simplicity. The longitudinal normal stress is assumed to be uniformly distributed over an effective flange width. However, in actual bridge cross-sections, the longitudinal normal stress in the deck is non-uniform, varying from maximum over the girder center-line to a minimum at the girder spacing center-line, due to in-plane shear flexibility of the deck, which is known as shear lag effect, as shown in Figure 1. The shear lag effect is a complex phenomenon as it depends on several factors such as cross sectional dimensions, stiffness of the deck and girder, and loading conditions (Chiewanichakorn, et al. 2004). In design practice, an effective flange width, which is defined as a reduced width based on center-to-center spacing of girders, is adopted to account for shear lag effect. For example, the current AASHTO Standard and LRFD Specifications (2008) provide provisions for effective flange width for concrete decks on steel girders with full-composite action. Based on a previous study (Moffatt and Dowling 1978), effective flange width

Journal of Bridge Engineering. Submitted March 10, 2011; accepted September 14, 2011;
posted ahead of print September 16, 2011. doi:10.1061/(ASCE)BE.1943-5592.0000308

is a significant factor to predict the deflections of the bridge and stresses in the flange for line girder analysis.

As of 2006, nearly 27.15% of the bridges in the US have been reported to be either structurally deficient or functionally obsolete (Status of the Nation's Highways, Bridges, and Transit: Conditions and Performance 2008). Hence, there is a need to explore new materials to enhance the durability and efficiency of structural bridge systems. Fiber Reinforced Polymer (FRP) composites have begun to play a key role in new construction and rehabilitation because of their high strength, light weight, favorable durability, and high corrosion resistance. In particular, FRP decks have been increasingly used in the US since the 1990's. The behavior of an FRP deck depends significantly on the type of shear connection used between the deck and supporting girders, which defines the degree of deck-girder composite action achieved. If there is no composite action in the system, slipping usually occurs between the two surfaces. As composite action increases, the slippage decreases until it becomes zero, representing full-composite action.

Although extensive research has been conducted on stiffness and strength evaluations of various types of FRP deck panels (e.g., Bakis, et al. 2002; Davalos and Chen, 2005; Chen and Davalos 2007; Chen and Davalos 2010), there are only limited studies available for effective flange width accounting for partial composite action and ortrotropic properties of the deck. Several researchers attempted to achieve a full-composite action for FRP deck bridge systems. Among others, based on a study of FRP deck-on-steel girder bridges in Pennsylvania, Keelor et al. (2004) reported that FRP decks acting compositely with underlying steel girders exhibited an effective width, at the service condition, of approximately 75% of the girder spacing for interior girders and 90% of the total distance, made up of the girder spacing added to the deck overhang,

Journal of Bridge Engineering. Submitted March 10, 2011; accepted September 14, 2011;
posted ahead of print September 16, 2011. doi:10.1061/(ASCE)BE.1943-5592.0000308

for the case of exterior girders. Turner et al. (2004) presented initial baseline results for a glass FRP (GFRP) deck system based on an in-situ testing. Critical design criteria, such as overall deflections, effective deck width, bending of the GFRP deck and moment distribution factors were reported. Moses et al. (2006) presented a number of in-situ tests of GFRP decks in South Carolina, Pennsylvania, and Ohio and addressed the development of appropriate LRFD design parameters for such deck systems. Mechanical shear connector with an enclosed grout area was used in these studies. It was reported that the composite behavior of FRP decks could be observed to degrade significantly in a few short years. While composite behavior may be quite appropriate at service limit states, it may not be appropriate at ultimate limit states. This was probably because of cracking and degradation of the grout, which could occur within a short time or under high stress concentration, causing a negative impact on the integrity of the deck and connection. Keller and Gurtler (2005a) conducted lab tests on two large scale T-sections to study composite action and effective flange width. Each test model was 7.5 m long with a pultruded FRP deck section of 1.5 m wide adhesively bonded to the top flange of a steel supporting beam. The normal strain distribution across the width of the FRP section was recorded at both top and bottom FRP facesheets. The results showed that under service limit state, the normal stress was almost uniform across the panel section. While under failure limit state, the normal stress decreased towards the panel edges, indicating a more pronounced effect of shear lag. Keller and Gurtler (2005b) studied the quasi-static and fatigue performance of hybrid bridge girders composed of cellular FRP bridge decks and steel girders, where the FRP bridge deck was connected adhesively to the steel girders. The results indicated that composite action could be achieved with the adhesive connection, and the well-established design method for steel-concrete composite girders with shear connections can essentially be used for the design of such FRP-

Journal of Bridge Engineering. Submitted March 10, 2011; accepted September 14, 2011;
posted ahead of print September 16, 2011. doi:10.1061/(ASCE)BE.1943-5592.0000308

steel girders. In both studies, a pronounced vertical shear lag effect was observed through the thickness of the FRP deck. In another study, Keller and Gurtler (2006) presented prediction methods for axial stresses and deflections at the serviceability limit state and for ultimate failure load.

However, full-composite action is usually difficult to achieve, and it may induce an adverse effect on the bridge system if the shear connection is fully constrained, because of the inconsistent thermal coefficient of expansion between FRP and steel. Partial composite action is more practical for FRP decks, and allows for thermal displacements of the FRP deck. Davalos et al. (2011) and Righman et al. (2004) developed a mechanical shear connector, which was successfully implemented in a scaled bridge test. This connection can prevent lifting of the FRP deck, and offers versatility of application to most FRP decks, ease of installation and replacement, and structural efficiency. This shear connector can achieve partial composite action, allowing relative displacement between the deck and supporting girders to account for thermal effects. Since grout is not required for this connector, it is expected that the composite action will not be affected by high stress, and acceptable performance over time can be expected. Based on limited data, Davalos et al. (2011) proposed an equation to estimate effective flange width for a given Degree of Composite Action (DCA).

Since no design guidelines are available to calculate effective flange width for FRP deck-on-steel girder bridges for partial composite action, and the design is usually based on non-composite action. The FRP deck is neglected in the stiffness and strength calculations, resulting in over-design of the supporting girders. Therefore, the objective of this study is to define the effective flange width for honeycomb FRP sandwich deck-on-steel girder systems, with either full or partial composite action, and propose design guidelines.

Journal of Bridge Engineering. Submitted March 10, 2011; accepted September 14, 2011;
posted ahead of print September 16, 2011. doi:10.1061/(ASCE)BE.1943-5592.0000308

In this paper, a Finite Element (FE) model is first developed to predict effective flange width for FRP deck-on-steel girder system with partial composite action, based on a proper definition of existing equations to calculate effective flange width, which is then verified by testing results of a T-beam section. The FE model is then used to carry out a parametric study by varying the DCA and stiffness of the bridge deck. Based on the results from the parametric study, a modified AASHTO equation is proposed to calculate the effective flange width. Finally, an example is provided to illustrate the use of the proposed equation. Since the FE model is based on the testing results for a T-beam section, the experimental testing is described first.

Test Description

Tests on a scaled FRP deck-on-steel girder bridge model were conducted to evaluate effective flange width, as briefly described below, and further details of the testing procedures are provided in Zou (2008) and Davalos et al. (2011).

Bridge Model Description

A one-third scaled bridge model with a span of 5.5 m was constructed consisting of three steel girders (W16x36, Gr50) spaced at 1.22 m on center (Figures 2a and 2b). A 5.5 m x 2.74 m x 0.13 m FRP deck was used, consisting of three 1.8 m wide by 2.74 m long individual FRP honeycomb panels from Kansas Structural Composite Inc. (KSCI), which were assembled using tongue-and-groove connections along the two 2.74 m transverse joints. The deck was attached to the girders using a prototype stud-sleeve connector (Davalos et al., 2011). The longitudinal direction of the honeycomb core (Figure 3) was perpendicular to the traffic direction.

Journal of Bridge Engineering. Submitted March 10, 2011; accepted September 14, 2011;
posted ahead of print September 16, 2011. doi:10.1061/(ASCE)BE.1943-5592.0000308

T-section Model Description and Test Setup

After completion of a series of static and fatigue tests on the scaled bridge, a T-section was cut-out from the center portion of the bridge to study its effective flange width. This section had a flange width of 1.22 m, as illustrated in Figures 2b and 4, which was longitudinally supported by a center steel girder. Three brackets were placed on each side of the flange to provide lateral support to the flange section. A patch load was applied at the mid-span of the T-beam over an area of 0.6x0.25 m^2 using a 490 kN actuator, as shown in Figure 4. The system was subjected to three-point bending with displacement control at a rate of 1 mm/min within service load limit, and load-displacement relation was recorded, as shown in Figure 5. As reported by Davalos et al. (2011), a 25% composite action could be achieved for this bridge system.

Finite Element Model

An FE model was created to simulate the T-beam section described above, as shown in Figure 6. The T-beam specimen consisted of a 1220 mm wide section of FRP deck attached to a W16x36 (American Institute of Steel Construction, Inc. 2005) steel girder. The deck was 130 mm thick, and the longitudinal span was 5500 mm.

The commercial FE software package ABAQUS (Dassault Systèmes 2007) was adopted because of its relative ease of use as well as its generality and comprehensive capabilities. For the construction of this model, all forces are expressed in N and all dimensions are expressed in mm, and correspondingly all pressure units are expressed in N/mm^2, or MPa.

The steel was modeled as a linear elastic isotropic material with the modulus of elasticity equal to 200,000 MPa and the Poisson's ratio equal to 0.3 (American Institute of Steel

Journal of Bridge Engineering. Submitted March 10, 2011; accepted September 14, 2011;
posted ahead of print September 16, 2011. doi:10.1061/(ASCE)BE.1943-5592.0000308

Construction, Inc. 2005). The material properties of the FRP deck were obtained from Zou et al. (2011a) and Zou (2008) (Table 1), based on a stiffness analysis using homogenization theory.

The elements used consisted of 4-node general-purpose shell elements with reduced integration and hourglass control, and finite membrane strains. These elements in ABAQUS are commonly referred to as "S4R" elements (Dassault Systèmes 2007). The mesh consisted of 28 elements along the deck width, four elements along the beam flange, eight elements along the beam web height, and 45 elements along the length of the T-beam section. Overall, 1980 elements were used in the FE model shown in Figure 6. The selected mesh provided accurate results based on convergence studies. This particular element pattern was also selected in order to align vertically the nodes along the top flange of the beam with corresponding nodes on the FRP deck, in order to simulate the effect of partial composite action for the T-beam specimen.

The patch load on the physical test specimen consisted of a 600 mm x 250 mm area, which was applied over a 6-element by 5-element area in this FE model, as a pressure load over 30 elements. It should be noted, however, that the actual area of the 30 central elements is slightly larger than the actual patch load applied to the T-beam test specimen, as will be discussed later.

Since the T-beam specimen was simply supported, the bottom edges of the ends of the wide flange beam were restrained to represent a hinge-roller condition. Also, since the deck was restrained from lateral movement during T-beam tests (Figure 4), the side edges of the deck in the finite element model were also laterally restrained.

The most important characteristic of this model is to simulate the interaction between the FRP deck and the steel girder. This was achieved using multiple-point constraint connector elements (CONN3D2 in ABAQUS) among the common nodes over the center contact section

Journal of Bridge Engineering. Submitted March 10, 2011; accepted September 14, 2011;
posted ahead of print September 16, 2011. doi:10.1061/(ASCE)BE.1943-5592.0000308

between the top flange of the beam and the bottom of the deck. Each connector element extended between the center-line of the beam flange thickness and the center-line of the deck thickness. To conduct the parametric study, and partially to verify the FE model with experimental results, the following boundary conditions for the connector element were specified: (1) All three rotational degrees of freedom are coupled between the beam and the deck (no relative rotation); (2) the vertical displacement in the z-direction (Figure 6) is coupled (no relative displacements). In addition, for full-composite action, all three displacements are coupled (x, y, and z). For non-composite action, the in-plane displacements (x and y) are allowed. And for partial composite action, elastic displacements are prescribed in the x and y directions, by varying the elastic displacement constants, to simulate partial composite behavior between the deck and the girder.

Verification of Finite Element Model

From the T-beam test, it was determined that the bridge system displayed a DCA of 25% (Davalos, et al. 2011). Therefore, this DCA needed to be simulated in the FE model. The DCA can be calculated as (Park, et al. 2005):

$$DCA = \frac{N_p - N_0}{N_{100} - N_0} \tag{1}$$

where N_0, N_p, and N_{100} are distances from the bottom of the girder to strain intersection points for non-composite, partial composite, and full-composite actions, respectively, as defined in Figure 7. The definition is essentially the same as that adopted by the Americano Institute of Steel

Journal of Bridge Engineering. Submitted March 10, 2011; accepted September 14, 2011;
posted ahead of print September 16, 2011. doi:10.1061/(ASCE)BE.1943-5592.0000308

Construction (AISC), as shown in Figure 8, where x indicates the amount of the horizontal slip (Lorenz and Stockwell, 1984), as will be discussed later.

To achieve a DCA of 25%, the FE model was analyzed for both full-composite and non-composite action first, where N_{100} and N_0 can be calculated as 300.9 mm and 385.4 mm, respectively. Based on Equation (1), N_{25}, corresponding to 25% DCA, can be calculated as 364.3 mm. Next, the elastic spring stiffness of the connector element was iterated until the target N_{25} was obtained. The spring stiffness obtained was 3,800 N/mm for this case.

To verify the accuracy of the FE model described above, a load of 160 kN was applied to the FE model with 25% DCA. The magnitude of the load was selected such that the stresses and strains in the model were in the linear elastic range, as shown in Figure 5. The deflections from the T-beam test and FE analysis were 13.4 mm and 14.4 mm, respectively, with the FE result to be 7% higher, which is acceptable, and this small difference verifies the accuracy of the FE model.

Based on the component test of a single shear connector (Davalos et al. 2011), the elastic spring stiffness can be calculated as 1,600 N/mm. Using this value instead of the 3,800 N/mm obtained above, the deflection from the FE analysis was 15.0 mm, with a difference of 12% from the bridge testing result, which is reasonable because the shear connector performs slightly differently at the component level from the system level. Thus, using the value of 3,800 N/mm is justified in order to represent the system behavior and achieve 25% DCA, as obtained experimentally for the scaled bridge.

Journal of Bridge Engineering. Submitted March 10, 2011; accepted September 14, 2011;
posted ahead of print September 16, 2011. doi:10.1061/(ASCE)BE.1943-5592.0000308

Parametric Study

Using the FE model described above, a parametric study was conducted considering two parameters: DCA for the girder/deck interaction and bridge deck stiffness. Results from the parametric study will be used to develop an empirical equation to calculate the effective flange width.

Degree of Composite Action

The following DCA were considered in the FE model: 0%, 25%, 50%, 75%, and 100%. Table 2 presents the strain intersection point location for each DCA considered calculated from Equation (1). The stiffness of the connector element was iterated to achieve different DCA as described above, with values shown in Table 2. Once the correct deck/girder interaction was achieved corresponding to each DCA, stresses and strains were obtained. Based on the strains obtained, the slip x as shown in Figure 8 can be calculated for each DCA as shown in Table 2. Alternatively, the slip values in Table 2 can be used to calculate DCA based on the concept from Figure 8, and the DCAs are the same as those evaluated using Equation (1). Therefore, either of these two methods can be used for calculating DCA.

With stresses along the deck width at the top and bottom known, an expression used by Zou et al. (2011), as shown in Equation (2), was used to evaluate the effective flange widths for each case:

$$b_{eff} = \frac{\int_{-b/2}^{b/2} \sigma_x dx}{\sigma_{x\max}} \tag{2}$$

Journal of Bridge Engineering. Submitted March 10, 2011; accepted September 14, 2011;
posted ahead of print September 16, 2011. doi:10.1061/(ASCE)BE.1943-5592.0000308

where b_{eff} is the effective flange width for FRP deck-on-steel girder system based on a given DCA; b is the actual width of the flange; σ_x is normal stress as shown in Figure 1; and $\sigma_{x\ max}$ is the maximum normal stress based on the given DCA.

Figure 9 displays strain distribution along the deck width for 100% DCA, where vertical shear lag effect is observed, with a b_{eff} of 1083.8 mm and 414.7 mm for top and bottom facesheets, respectively, based on Equation (2). However, as pointed out by Moses et al. (2006), the effective flange width can be calculated by assuming that top and bottom facesheets contribute equally. The inherent assumption of this procedure is that all strains are in the elastic range, as shown in Figure 10 for 100% DCA, where linear strain distribution occurs through the depth of the FRP deck. Therefore, it is reasonable to use the average value of the stresses at top and bottom facesheets, σ_x, in Equation (2).

The actual width of the deck was composed of 28 elements as stated above, and therefore, 28 stresses can be obtained from the FE model. Based on Equation (2), effective flange widths for different DCA were calculated and listed in Table 3. It can be seen from Table 3 that effective flange widths were approximately the same except for 0% DCA, where no meaningful value can be calculated for 0% DCA since σ_x and $\sigma_{x\ max}$ are both zero. This is not reasonable since the DCA is an indication of the contribution to the composite section from the FRP deck. For 100% DCA, the whole FRP deck contributes to the composite section, where b_{eff} is the maximum. For 0% DCA, the FRP deck does not contribute to the composite section, where b_{eff} becomes 0. For other DCAs, b_{eff} varies between 0 and the maximum value. Therefore, Equation (2) is only valid for calculating effective flange width for full-composite action. It is recommended that Equation (2) be modified as shown in Equation (3), where the maximum

Journal of Bridge Engineering. Submitted March 10, 2011; accepted September 14, 2011;
posted ahead of print September 16, 2011. doi:10.1061/(ASCE)BE.1943-5592.0000308

stress $\sigma_{x\ max}$ in Equation (2) was replaced by the maximum stress corresponding to full-composite action, $\sigma_{x\ max\text{-}full\ composite}$ as

$$b_{eff} = \frac{\int_{-b/2}^{b/2} \sigma_x dx}{\sigma_{x\ \max - full\ composite}} \tag{3}$$

with all parameters defined in the same way as in Equation (2).

The maximum average compressive stress for full-composite action was calculated to be 2.99 MPa. Using Equation (3), the effective widths for each DCA were calculated as shown in Table 4 and Figure 11. It is noted that for full composite action, the effective flange width obtained in a previous study (Zou et al. 2011) for the same model was 1010 mm based on shear lag model, which is about 5% different from the value of 961.7 mm shown in Table 4. This can also validate the accuracy of the FE model developed above. A linear relationship between effective flange width and DCA can be observed in Figure 11 as:

$$b_{eff} = b_{eff - full\ compoiste} \times DCA \tag{4}$$

where b_{eff} and $b_{eff\text{-}full\ composite}$ are the effective flange width for FRP deck-on-steel girder system for a given DCA and full-composite action, respectively.

Bridge Deck Stiffness

The bridge deck stiffness was varied from a value representing the FRP material properties up to a value representing concrete material properties, at 20% increments, assuming

Journal of Bridge Engineering. Submitted March 10, 2011; accepted September 14, 2011;
posted ahead of print September 16, 2011. doi:10.1061/(ASCE)BE.1943-5592.0000308

full-composite action between the girder and deck. The relevant stress data were retrieved for each case and the effective widths were obtained in accordance with Equation (3), as shown in Table 5, which indicates that the deck stiffness has a negligible effect on the effective flange width. It is interesting to find out that significant shear lag effect is obtained even for a deck with equivalent concrete properties, which appears to be different from the concept in AASHTO Specifications, where no reduction factor is used when calculating the effective flange width. It is worth noting that in the current model, the deck is treated as an orthotropic plate, which is sufficient for FRP decks but cannot be directly applied to Reinforced Concrete (RC) decks, since the reinforcement inside the RC deck is not included. Detailed descriptions on modeling concrete decks can be found in Chiewanichakorn et al. (2004) and Ahn et al. (2004). It is expected that the reduction effect will be significant lower for RC decks.

Although the FE model developed above is based on a scaled bridge system from a full-scale bridge model, it essentially represents an FRP deck on steel girder bridge. Based on past experience with the effective flange width and load distribution factor (Zou et al. 2011a; Zou et al. 2011b), where both scaled-bridge and full-bridge models were considered, the scaled effect seems to have negligible effect on the results. Therefore, the results will be used to develop a design equation for FRP deck over interior girders, as will be shown next.

Design Equation of Effective Flange Width for FRP deck over Interior Steel Girders

AASHTO Specifications (2008) provide the following guidelines for determining the effective flange width to be used in design for interior girders:

- ¼ the effective span length;

Journal of Bridge Engineering. Submitted March 10, 2011; accepted September 14, 2011;
posted ahead of print September 16, 2011. doi:10.1061/(ASCE)BE.1943-5592.0000308

- 12.0 times the average thickness of the slab, plus the greater of the web thickness OR ½ the width of the top flange of the girder; and
- the average spacing of adjacent beams.

The controlling effective flange width shall be taken as the minimum of the above values. It should be noted that these guidelines are for the consideration of full-composite action of the deck and girder system. For the T-beam section described above, the controlling effective width in accordance with AASHTO Specifications is the average spacing of the girders (1220 mm). The effective flange width for full-composite action using the average stresses as presented in Equation (3) is determined to be 962 mm. Therefore,

$$\frac{b_{eff-full\ composite(FRP\ Deck)}}{b_{eff\ AASHTO}} = \frac{962\ mm}{1220\ mm} = 0.79 \tag{5}$$

Based on experimental field testing, several researchers reported reduction factors for different types of FRP decks, as shown in Table 6. Therefore, a reduction factor is recommended to be applied to AASHTO specified values for calculating effective flange width of FRP deck-on-steel girders as:

$$b_{eff-full\ composite} = b_{eff\ AASHTO} \times RF \tag{7}$$

where $b_{eff\text{-}full\ composite}$ is the effective flange width for FRP deck-on-steel girder system with full-composite action; $b_{eff\ AASHTO}$ is effective flange width calculated from AASHTO Specifications; and RF is a reduction factor. Based on Equations (5), it seems to be reasonable to assume

Journal of Bridge Engineering. Submitted March 10, 2011; accepted September 14, 2011;
posted ahead of print September 16, 2011. doi:10.1061/(ASCE)BE.1943-5592.0000308

RF=0.75 for the honeycomb FRP sandwich deck connected to the steel girder using a mechanical shear connector studied in this paper. Further study is still needed in order to determine the *RF* for different types of FRP decks and connectors.

Substituting Equation (8) into Equation (4), we have

$$b_{eff} = b_{eff\ AASHTO} \times RF \times DCA \tag{8}$$

with all parameters defined in the same way as in Equation (7).

Example

An example is provided to illustrate the use of the proposed Equation (8) and the benefits on stiffness and strength by incorporating FRP deck in the design. The configuration of the example bridge is described below based on a preliminary design (Figure 12):

1. Simply supported 21.33 m (70 ft) span.
2. 10.97 m (36 ft) wide accommodating two design lanes.
3. Five W40x199 Grade 50 rolled steel girders at 2.44 m (8 ft) on centers, with a yielding strength f_y=345 MPa.
4. 254 mm (10 in) thick FRP honeycomb sandwich deck panel connected to steel girders using the shear connection as described in Davalos et al. (2011). Therefore, the bridge has 25% DCA.
5. The deck configuration is shown in Figure 13. The properties of facesheet and core material are listed in Tables 7 through 9. The equivalent properties of FRP panel are

Journal of Bridge Engineering. Submitted March 10, 2011; accepted September 14, 2011;
posted ahead of print September 16, 2011. doi:10.1061/(ASCE)BE.1943-5592.0000308

listed in Table 10. Detailed procedures to obtain the equivalent engineering properties of this FRP panel can be found in Davalos *et al.* (2001).

6. Compressive strength of the facesheet is 2.43 kN/mm (13.9 kips/inch) provided by Chen (2004). It is assumed that the full face plate capacity can be achieved since the failure strain for the FRP plate is 0.015, which is significantly lower than the plastic strain for steel, which is around 0.2.

Step 1. Effective Flange Width

For interior girders, the effective flnage width for concrete deck based on AASHTO Specification (2008) is the smaller value of :

1. ¼ the effective span length: 0.25x21330=5333 mm
2. 12 times the average thickness of the slab, plus the greater of the web thickness or ½ the width of the top flange of the girder: 12x254+201=3249 mm
3. The average spacing of adjacent beams: 2440 mm

Therefore, $b_{eff\ AASHTO}$=2440 mm. Substituting this value into Equation (10), we have:

$$b_{eff} = b_{eff\ AASHTO} \times RF \times DCA = 2440 \times 0.75 \times 25\% = 457\ mm \tag{9}$$

Step 2. Section Properties

The 25% DCA partial composite section properties are calculated in Table 12, based on dimensions shown in Table 11 and Figure 14(a). The modular ratio of n is calculated as

$$n = \frac{E_{steel}}{(E_y)_{deck}} = \frac{200\ GPa}{1.475\ GPa} = 136 \tag{10}$$

Therefore, the transformed width of the FRP deck is

Journal of Bridge Engineering. Submitted March 10, 2011; accepted September 14, 2011;
posted ahead of print September 16, 2011. doi:10.1061/(ASCE)BE.1943-5592.0000308

$$b_{transformed} = \frac{b_{eff}}{n} = \frac{457}{136} = 3.4\ mm \tag{11}$$

The centroid of the section is calculated from the top of the FRP deck as:

$$\bar{y}_{NA} = \frac{2.818 \times 10^7}{38534} = 731\ mm \tag{12}$$

The parallel axis theorem is used to get the moment of inertia of the components about this centroid, as shown in Table 12.

Step 3. Nominal Plastic Moment Capacity M_n

The plastic moment considering contribution from FRP deck and steel girder can be calculated based on dimensions shown in Figure 14(b) and Table 11. By inspection, the Plastic Neutral Axis (PNA) lies in the web of the steel beam, which is located a distance $\bar{y}_{PNA}$ from the top of the deck. $\bar{y}_{PNA}$ can be calculated to be 522 mm. Therefore,

- Tension Flange:

$$\text{Force: } P_{ft} = F_y b_f t_f = (345)(400)(27) = 3731\ kN \tag{13}$$

$$\text{Moment arm: } d_{ft} = 673\ mm$$

- Compression Flange:

$$\text{Force: } P_{fc} = F_y b_f t_f = (345)(400)(27) = 3731\ kN \tag{14}$$

$$\text{Moment arm: } d_{fc} = 282\ mm$$

- Tension Web:

$$\text{Force: } P_{wt} = F_y b_{wt} t_w = (345)(660)(17) = 3754\ kN \tag{15}$$

$$\text{Moment arm: } d_{wt} = 330\ mm$$

- Compression Web:

Journal of Bridge Engineering. Submitted March 10, 2011; accepted September 14, 2011;
posted ahead of print September 16, 2011. doi:10.1061/(ASCE)BE.1943-5592.0000308

Force: $P_{wc} = F_y b_{wc} t_w = (345)(268)(17) = 1528\ kN$

Moment arm: $d_{wc} = 134\ mm$ (16)

- FRP Deck:

Force: $P_d = 2F_d b_{eff} = (2)(2434)(457) = 2226\ kN$

Moment arm: $d_d = 423\ mm$ (17)

where F_d is the compressive strength of the facesheet (Chen, 2004), and b_{eff} is the effective flange width. It is assumed that the compressive force is carried by the two facesheets only.

The plastic moment is the sum of the moments of the plastic forces about the PNA.

$$M_P = P_{ft} d_{ft} + P_{fc} d_{fc} + P_{wt} d_{wt} + P_{wc} d_{wc} + P_d d_d = 4.956 \times 10^5\ kN - mm \quad (18)$$

Moment of inertial I_x and nominal plastic moment capacity M_n for other DCA can be calculated following the same procedures, with results shown in Table 13.

Discussions

It can be seen from Table 13 that an FRP deck with a low stiffness can still contribute to the stiffness and strength of the system. As illustrated from this example, with 25% DCA and *n=136* (*n=6~10* for normal weight concrete), the stiffness and strength can be increased by 5% and 21%, respectively. Therefore, it is advantageous to include FRP deck in design by properly considering its DCA. It is also interesting to find out that DCA between 25% to 50% seems to give an optimum performance since the gain of the strength becomes less significant beyond 50% DCA. This partial composite action can also provide relative slip to account for the differences of the coefficients of thermal expansion between FRP deck and steel girders.

Journal of Bridge Engineering. Submitted March 10, 2011; accepted September 14, 2011;
posted ahead of print September 16, 2011. doi:10.1061/(ASCE)BE.1943-5592.0000308

Conclusions

This paper systematically studies the effective flange width for honeycomb FRP sandwich deck with sinusoidal core geometry-on-steel girder bridge system using a mechanical shear connector with full or partial composite actions. Based on this study, the following conclusions can be drawn:

1. The FE model developed in this paper can accurately describe the performance of FRP deck-on-steel girder bridge system with partial composite action, with favorable correlations between the FE and testing results.
2. A parametric study was conducted using the FE model by considering different degrees of composite action and stiffness of bridge decks. Based on the parametric study, an empirical equation was proposed to calculate effective flange width for different degrees of composite action. Bridge deck stiffness has a negligible effect on the effective flange width.
3. The concept of the effective flange width can be redefined for partial composite action, by dividing the normal stress resultant by the maximum normal stress corresponding to full-composite action, instead of the maximum normal stress for the specific degree of composite action.
4. The AASHTO guidelines can be modified for FRP deck with partial composite action for interior girders by incorporating an appropriate reduction factor.
5. Although the stiffness of the FRP deck is low, it can still contribute significantly to the stiffness and strength of the bridge system, even with a partial composite action. This is in contrast to the general impression that, because of the low

Journal of Bridge Engineering. Submitted March 10, 2011; accepted September 14, 2011;
posted ahead of print September 16, 2011. doi:10.1061/(ASCE)BE.1943-5592.0000308

equivalent modulus of the FRP deck, the contribution of the deck to the bridge system is not significant even with full-composite action.

This paper presents a method for studying effective flange width for FRP deck-on-steel girder system with partial composite action. Further studies need to be conducted including more tests to verify the findings from this paper, and applying this method to study effective flange width for different types of FRP decks and for exterior girders.

References

Ahn, I., Chiewanichakorn, M., Chen, S. S., and Aref, A. J. (2004). "Effective Flange Width Provisions for Composite Steel Bridges," *Engineering Structure*, 26, pp. 1843-1851.

American Association of State Highway and Transportation Officials. *AASHTO LRFD Bridge Design Specifications, Fourth Edition (with 2008 revisions).* Washington, DC: AASHTO, 2008.

American Institute of Steel Construction, Inc. *Steel Construction Manual, 13th Edition.* AISC, 2005.

Bakis, C.E., Bank, L.C., Brown, V.L., Cosenza, E, Davalos, J.F., Lesko, J.J., Machida, A., Rizkalla, S.H., and Triantafillou, T.C. (2002). "Fiber-reinforced Polymer Composites for Construction-State-of-Art Review," *Journal of Composites for Construction*, ASCE, 6(2), pp. 73-87.

Chen, A. (2004). *Strength evaluation of honeycomb FRP sandwich panels with sinusoidal core geometry,* PhD Dissertation, West Virginia University, Morgantown, WV

Chen, A. and Davalos, J.F. (2007). "Transverse Shear with Skin Effect for Composite Honeycomb Sinusoidal Core Sandwich," *Journal of Engineering Mechanics, ASCE*, 133(3), pp. 247-256.

Chen, A. and Davalos, J.F. (2010). "Strength Evaluations of Sinusoidal Core for FRP Sandwich Bridge Deck Panels," *Composite Structures*, 92(7), pp. 1561-1573.

Chiewanichakorn, M., Aref, A.J., Chen, S.S., and Ahn, I.S. (2004) "Effective Flange Width Definition for Steel-Concrete Composite Bridge Girder." *Journal of Structural Engineering*, 130(12), pp. 2016-2031.

Dassault Systèmes. *ABAQUS/CAE User's Manual, Version 6.7.* Pawtucket, RI, 2007.

Journal of Bridge Engineering. Submitted March 10, 2011; accepted September 14, 2011;
posted ahead of print September 16, 2011. doi:10.1061/(ASCE)BE.1943-5592.0000308

Davalos, J.F. and Chen, A. (2005). "Buckling Behavior of Honeycomb FRP Core with Partially Restrained Loaded Edges under Out-of-plane Compression," *Journal of Composite Materials*, 39(16), pp. 1465-1485.

Davalos, J.F., Chen A., and Zou, B. (2011), "Stiffness and Strength Evaluations of a New Shear Connection System for FRP Bridge Decks to Steel Girders," accepted by *Journal of Composite for Construction, ASCE*, in press. (available online)

Davalos, J.F., P.Z. Qiao, X.F. Xu, J. Robinson, and K.E. Barth (2001), "Modeling and Characterization of Fiber-reinforced Plastic Honeycomb Sandwich Panels for Highway Bridge Applications", *Composite Structures*, 52, pp. 441-452.

Keelor, D.C., Luo, Y., Earls, C.J., and Yulismana, W. (2004). "Service Load Effective Compression Flange Width in Fiber Reinforced Polymer Deck Systems Acting Compositely with Steel Stringers." *Journal of Composites for Construction*, 8(4), pp. 289-297.

Keller, T., Gurtler, H. (2005). "Composite Action and Adhesive Bond between Fiber-Reinforced Polymer Bridge Decks and Main Girders," *Journal of Composites for Construction*, 9(4), pp. 360-368.

Keller, T. and Gürtler, H. (2005a). " Composite Action and Adhesive Bond between Fiber-Reinforced Polymer Bridge Decks and Main Girders," *Journal of Composites for Construction*, 9(4) pp. 360-368.

Keller, T. and Gürtler, H. (2005b). "Quasi-static and fatigue performance of a cellular FRP bridge deck adhesively bonded to steel girders," *Composite Structures*, 70(4), pp. 484-496.

Keller, T. and Gürtler, H. (2006). "Design of hybrid bridge girders with adhesively bonded and compositely acting FRP deck," *Composite Structures* 74(2), pp. 202-212.

Lorenz, R. F. and Stockwell, F. W. (1984). "Concrete Slab Stresses in Partial Composite Beams and Girders,"*AISC Engieering Journal*, 3rd Quarter, pp. 185-188.

Moffatt, K.R., and Patrick J.D. (1978). "British Shear Lag Rules for Composite Girders." *Journal of the Structural Division*, 104(7), pp. 1123-1130.

Moses, J. P., Harries, K. A., Earls, C. J., and Yulismana, W. (2006). " Evaluation of Effective Width and Distribution Factors for GFRP Bridge Decks Supported on Steel Girders," *Journal of Bridge Engineeing, ASCE,* 11(4), pp. 401-409.

Park, K.T., Kim, S.H., Lee, Y.H., and Hwang Y.K. (2005). "Degree of Composite Action Verification of Bolted GFRP Bridge Deck-to-Girder Connection System." *Composite Structures*, 72, pp. 393-400.

Journal of Bridge Engineering. Submitted March 10, 2011; accepted September 14, 2011;
posted ahead of print September 16, 2011. doi:10.1061/(ASCE)BE.1943-5592.0000308

Righman, J., Barth, K.E., and Davalos, J.F. (2004). "Development of an Efficient Connector System for Fiber Reinforced Polymer Bridge Decks to Steel Girders," *Journal of Composites for Construction*, 8(4), pp. 279-288.

Turner, M. K., Harries, K. A., Petrou, M. F., and Rizos, D. (2004). "In situ structural evaluation of a GFRP bridge deck system," *Composite Structures*, 65, pp. 157-165.

"Status of the Nation's Highways, Bridges, and Transit: Conditions and Performance." *Federal Highway Administration.* 2008. http://www.fhwa.dot.gov/policy/2008cpr/chap3.htm#8.

Yulismana, W. (2005). "*Experimental Study of the Behavior of Fiber Reinforced Polymer Deck System,"* Ph.D. Dissertation, University of Pittsburgh, Pittsburgh, PA.

Zou, B. (2008). "*Design Guidelines for FRP Honeycomb Sandwich Bridge Decks,*" Ph.D. Dissertation, West Virginia University, Morgantown, WV, USA

Zou, B., Chen, A., Davalos, J.F. and Salim, H.A. (2011a). "Evaluation of Effective Flange Width by Shear Lag Model for Orthotropic FRP Bridge Decks," Composite Structures, 93, pp. 474-482.

Zou, B., Davalos, J.F., **Chen, A.**, and Ray, I. (2011b). "Evaluation of Load Distribution Factor by Series Solution for Orthotropic Bridge Decks," *Journal of Aerospace Engineering, ASCE,* 24(2), pp. 227-239. (lead/corresponding author)

Journal of Bridge Engineering. Submitted March 10, 2011; accepted September 14, 2011;
posted ahead of print September 16, 2011. doi:10.1061/(ASCE)BE.1943-5592.0000308

Table 1 : Equivalent Properties of FRP Panel

E_x (MPa)	E_y (MPa)	ν_x (MPa)	G_{xy} (MPa)
5640	5640	0.303	1400

Table 2: FE Parameters

Degree of Composite Action	100%	0%	25%	50%	75%
Strain Intersection Point Measured from the Bottom of the Girder (mm) (See Figure 7)	300.9	385.4	364.4	343.2	322.1
Spring Stiffness (N/mm)	∞	0	3,800	12,300	43,500
Strain Slip ($x10^{-6}$) (See Figure 8)	0	1,474	1,102	733	370

Table 3: Effective Flange Widths from Eq. (2)

Degree of Composite Action	0%	25%	50%	75%	100%
Effective Flange Width (mm)	N/A	989.3	1047.8	1023.4	961.7

Table 4: Effective Flange Widths from Eq. (3)

Degree of Composite Action	0%	25%	50%	75%	100%
Effective Flange Width (mm)	0	235.6	501.9	746.6	961.7

Table 5: Effective Flange Width – Varying Deck Stiffness

% FRP to Concrete	Max Average Stress (MPa)	Effective Width (mm)
20	3.48	989.5
40	3.70	994.0
60	3.81	995.1
80	3.88	995.4
100	3.91	995.4

Journal of Bridge Engineering. Submitted March 10, 2011; accepted September 14, 2011;
posted ahead of print September 16, 2011. doi:10.1061/(ASCE)BE.1943-5592.0000308

Table 6: Reduction Factor For Different Bridge Deck

Bridge Deck	Reduction Factor		Source
	Interior Girder	Exterior Girder	
DuraSpan	0.75	0.9	Keelor et al. (2004)
DuraSpan	0.75	-	Keller and Gurtler (2005a)
DuraSpan	0.71-0.88	0.71-0.92	Moses et al. (2004)
DuraSpan	0.62-0.96		Turner et al. (2004)[1]
ASSET	1	-	Keller and Gurtler (2005b)

Note 1: Results do not separate interior and exterior girders.

Table 7: Material Properties of Facesheet

		Nominal Weight (g/m^2)	Thickness(mm)	V_f
CM 3205	0° or 90°	542.5	0.62	0.3428
	ContSM	152.6	0.254	0.2359
UM 1810	0°	610.3	0.635	0.3774
	ContSM	305.2	0.335	0.3582
Bonding Layer	ChopSM	600	3.175	0.1726

Table 8: Stiffness Properties of Facesheet Lamina

	Orientation	$E_1(GPa)$	$E_2(GPa)$	$G_{12}(GPa)$	$G_{23}(GPa)$	ν_{12}	ν_{23}
CM 3205	0° or 90°	27.72	8.00	3.08	2.88	0.295	0.390
	Random	11.79	11.79	4.21	2.36	0.402	0.400
UM 1810	0°	30.06	8.55	3.30	3.08	0.293	0.386
	Random	15.93	15.93	5.65	2.96	0.409	0.388
Bonding Layer	Random	9.72	9.72	3.50	2.12	0.394	0.401

Table 9: Stiffness Properties of Facesheet and Core

	$E_x(GPa)$	$E_y(GPa)$	ν_x	$G_{xy}(GPa)$
Facesheet	19.3	12.35	0.32	3.812
Core	0.529	0.000986	0.431	0.000705

Journal of Bridge Engineering. Submitted March 10, 2011; accepted September 14, 2011;
posted ahead of print September 16, 2011. doi:10.1061/(ASCE)BE.1943-5592.0000308

Table 10: Equivalent Properties of FRP Panel

	$E_x(GPa)$	$E_y(GPa)$	ν_x	$G_{xy}(GPa)$
In-Plane	2.747	1.475	0.321	0.741
Bending	6.417	3.896	0.32	1.422

Table 11: Dimensions of W40x199

Designation	Area (mm^2)	Depth d (mm)	Web Thickness t_w (mm)	Flange		Moment of Inertia I (mm^4)	Plastic Modulus Z_x (mm^3)
				Width b_f (mm)	Thickness t_f (mm)		
W 40x199	37677	982	17	400	27	6.202E+9	1.422E+07

Table 12: Partial Composite Section Properties (n=136, DCA=25%)

Component	Transformed Width (mm)	Area (mm^2)	y (mm)	Ay (mm^3)	$A(y-\bar{y}_{NA})^2$ (mm^3)	I_0 (mm^4)	I_x (mm^4)
FRP Deck	3.4	857	127	1.088E+05	1.232E+07	4.607E+06	3.176E+08
Steel		37677	745	2.807E+07	2.803E+05	6.202E+09	6.209E+09
Sum		38534		2.818E+07			6.527E+09

Table 13: Moment of Inertial I and Nominal Plastic Moment Capacity M_n vs. DCA

DCA	0	25%	50%	75%	100%
Ix (mm^4)	6.202E+09	6.527E+09	6.837E+09	7.135E+09	7.421E+09
I/I_{steel}	1.00	1.05	1.10	1.15	1.20
M_n (kN-mm)	4.086E+05	4.956E+05	5.559E+05	5.613E+05	5.826E+05
$M_n/M_{n\text{-}steel}$	1.00	1.21	1.36	1.37	1.43

Journal of Bridge Engineering. Submitted March 10, 2011; accepted September 14, 2011;
posted ahead of print September 16, 2011. doi:10.1061/(ASCE)BE.1943-5592.0000308

Figure 1: Effective Flange Width (Not to Scale)

Figure 2: Photo (a) and Details (b) of Scaled Bridge Model

Figure 3: KSCI honeycomb FRP panel

Figure 4: T-beam Test Model

Figure 5: T-beam Load vs. Deflection Data

Figure 6: FE Model

Figure 7: Strain Distribution for 100%, Partial, and 0% Composite Action

Figure 8: Partial Composite Action defined by AISC

Figure 9: Strain Distribution along the Width of the Bridge Deck (Full-Composite Action)

Figure 10: Strain Distribution along the Depth of the Girder and Bridge Deck (Full-Composite Action)

Figure 11: Effective Flange Width vs. DCA

Figure 12: Cross Section of the Example Bridge

Figure 13: FRP Deck Configurations

Figure 14: Partial Composite Sections

Figure 1

Journal of Bridge Engineering. Submitted March 10, 2011; accepted September 14, 2011; posted ahead of print September 16, 2011. doi:10.1061/(ASCE)BE.1943-5592.0000308

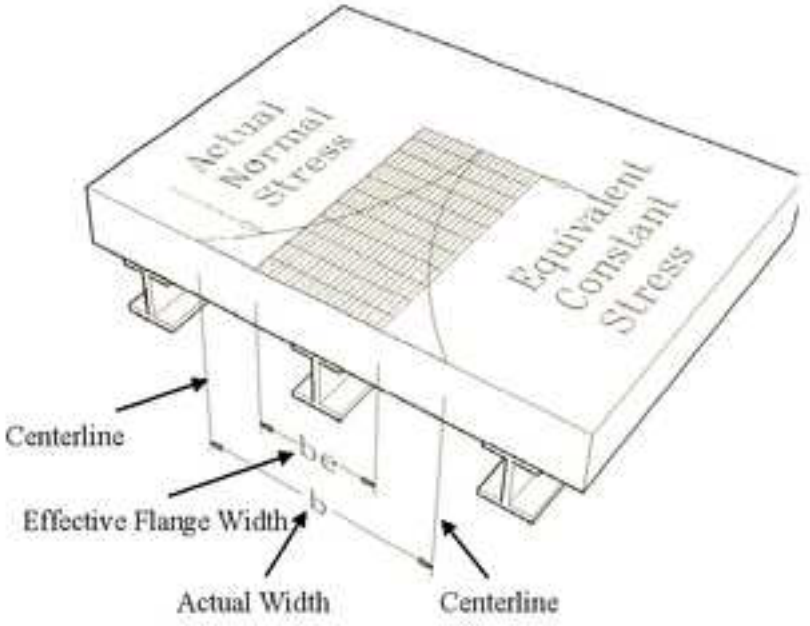

Figure 1: Effective Flange Width (Not to Scale)

Journal of Bridge Engineering. Submitted March 10, 2011; accepted September 14, 2011;
posted ahead of print September 16, 2011. doi:10.1061/(ASCE)BE.1943-5592.0000308

(a)

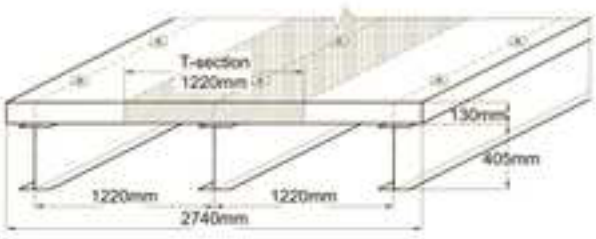

(b)

Figure 2: Photo (a) and Details (b) of Scaled Bridge Model

Journal of Bridge Engineering. Submitted March 10, 2011; accepted September 14, 2011; posted ahead of print September 16, 2011. doi:10.1061/(ASCE)BE.1943-5592.0000308

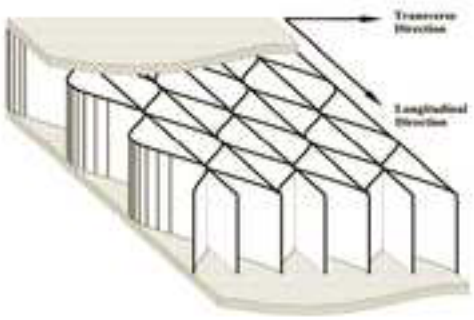

Figure 3: KSCI honeycomb FRP panel

Figure 4

Journal of Bridge Engineering. Submitted March 10, 2011; accepted September 14, 2011; posted ahead of print September 16, 2011. doi:10.1061/(ASCE)BE.1943-5592.0000308

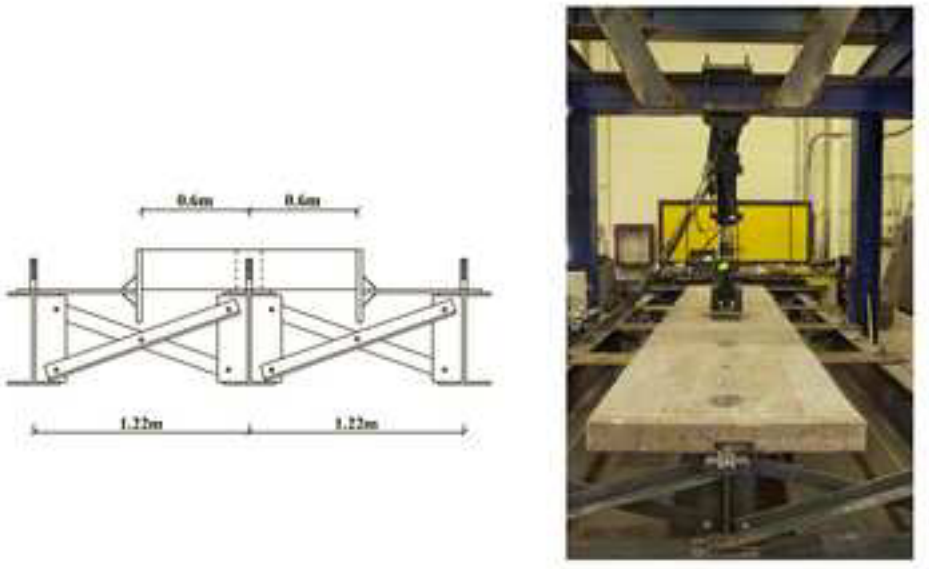

Figure 4: T-beam Test Model

Figure 5

Journal of Bridge Engineering. Submitted March 10, 2011; accepted September 14, 2011; posted ahead of print September 16, 2011. doi:10.1061/(ASCE)BE.1943-5592.0000308

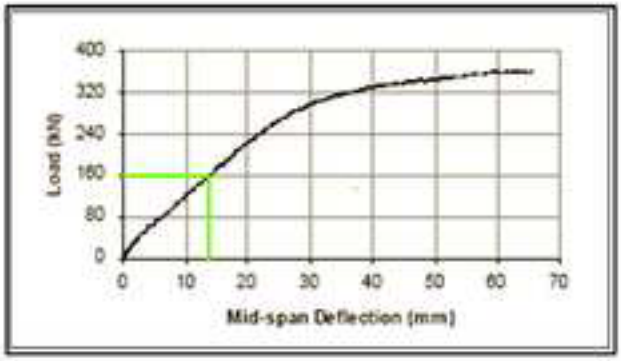

Figure 5: T-beam Load vs. Deflection Data

Figure 6

Journal of Bridge Engineering. Submitted March 10, 2011; accepted September 14, 2011;
posted ahead of print September 16, 2011. doi:10.1061/(ASCE)BE.1943-5592.0000308

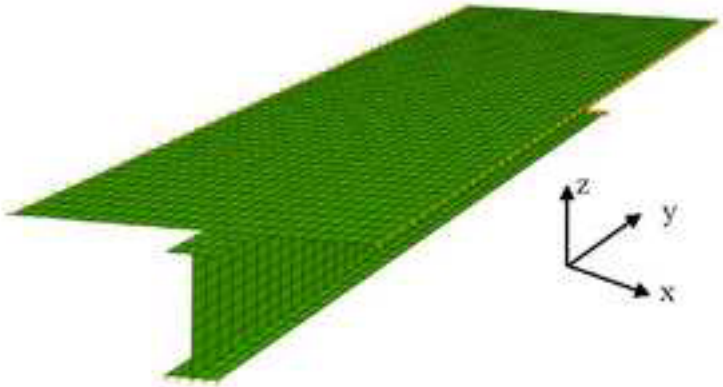

Figure 6: FE Model

Figure 7

Journal of Bridge Engineering. Submitted March 10, 2011; accepted September 14, 2011;
posted ahead of print September 16, 2011. doi:10.1061/(ASCE)BE.1943-5592.0000308

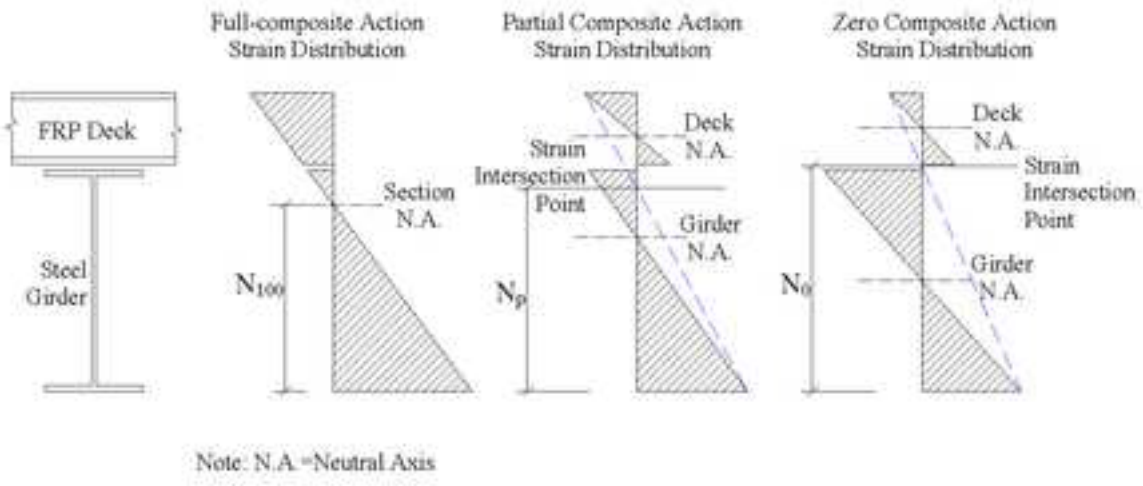

Figure 7: Strain Distribution for 100%, Partial, and 0% Composite Action

Figure 8

Journal of Bridge Engineering. Submitted March 10, 2011; accepted September 14, 2011; posted ahead of print September 16, 2011. doi:10.1061/(ASCE)BE.1943-5592.0000308

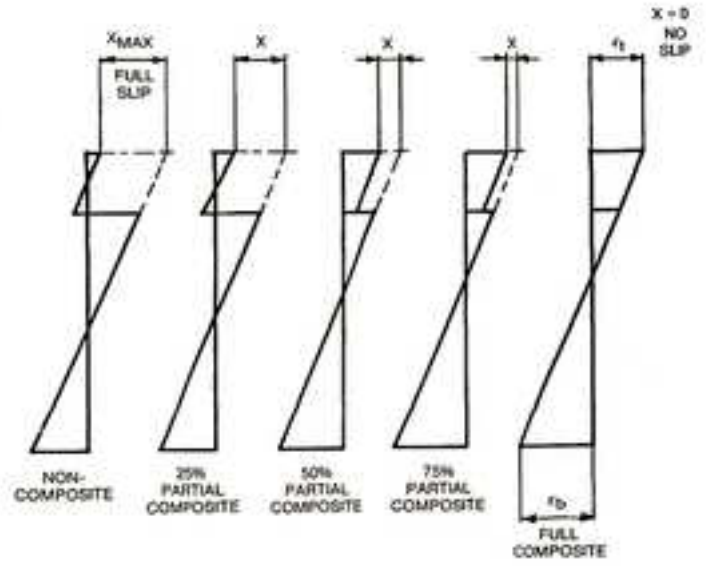

Figure 8: Partial Composite Action defined by AISC

Figure 9

Journal of Bridge Engineering. Submitted March 10, 2011; accepted September 14, 2011;
posted ahead of print September 16, 2011. doi:10.1061/(ASCE)BE.1943-5592.0000308

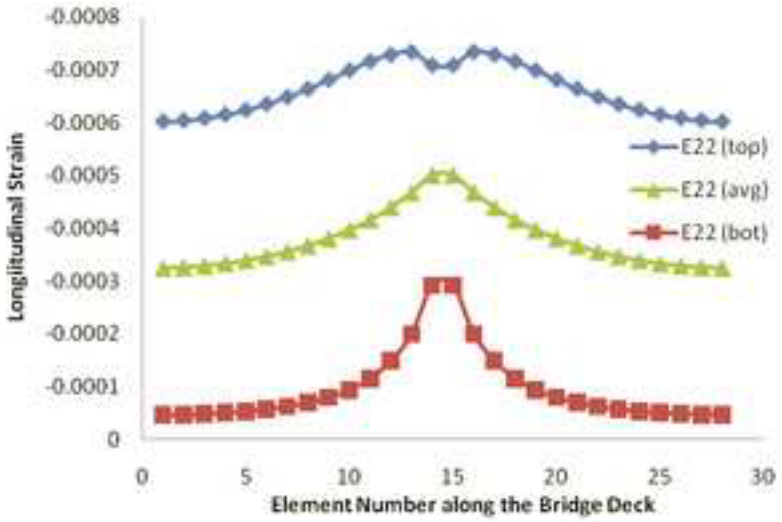

Figure 9: Strain Distribution along the Width of the Bridge Deck (Full-Composite Action)

Journal of Bridge Engineering. Submitted March 10, 2011; accepted September 14, 2011;
posted ahead of print September 16, 2011. doi:10.1061/(ASCE)BE.1943-5592.0000308

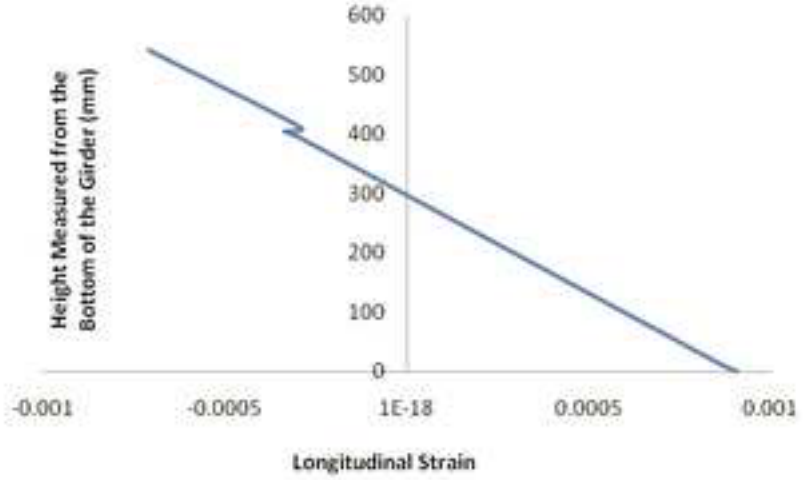

Figure 10: Strain Distribution along the Depth of the Girder and Bridge Deck (Full-Composite Action)

Journal of Bridge Engineering. Submitted March 10, 2011; accepted September 14, 2011; posted ahead of print September 16, 2011. doi:10.1061/(ASCE)BE.1943-5592.0000308

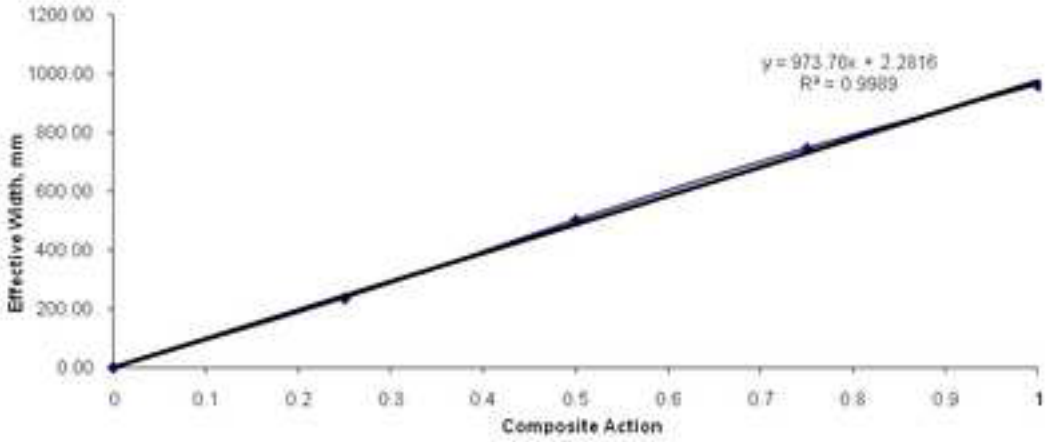

Figure 11: Effective Flange Width vs. DCA

Journal of Bridge Engineering. Submitted March 10, 2011; accepted September 14, 2011; posted ahead of print September 16, 2011. doi:10.1061/(ASCE)BE.1943-5592.0000308

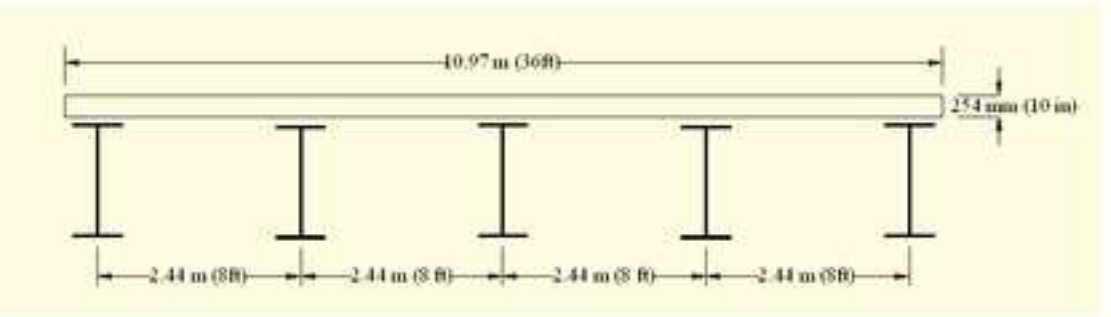

Figure 12: Cross Section of the Example Bridge

Journal of Bridge Engineering. Submitted March 10, 2011; accepted September 14, 2011;
posted ahead of print September 16, 2011. doi:10.1061/(ASCE)BE.1943-5592.0000308

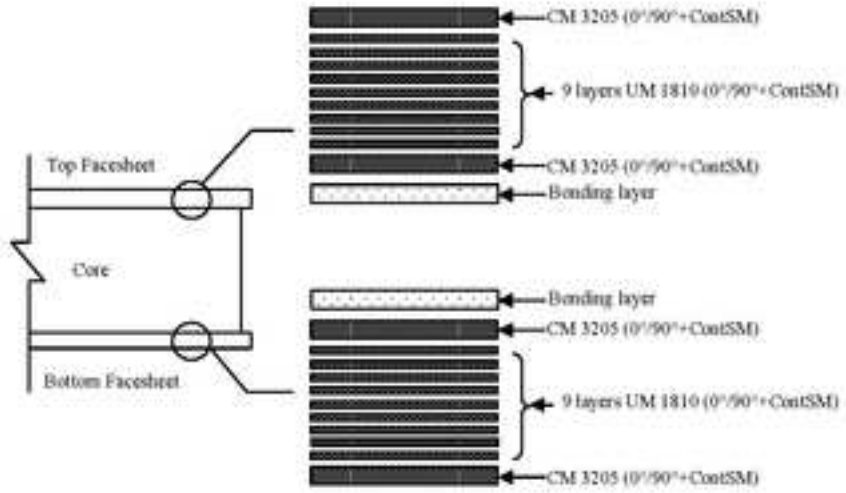

Figure 13: FRP Deck Configurations

Journal of Bridge Engineering. Submitted March 10, 2011; accepted September 14, 2011; posted ahead of print September 16, 2011. doi:10.1061/(ASCE)BE.1943-5592.0000308

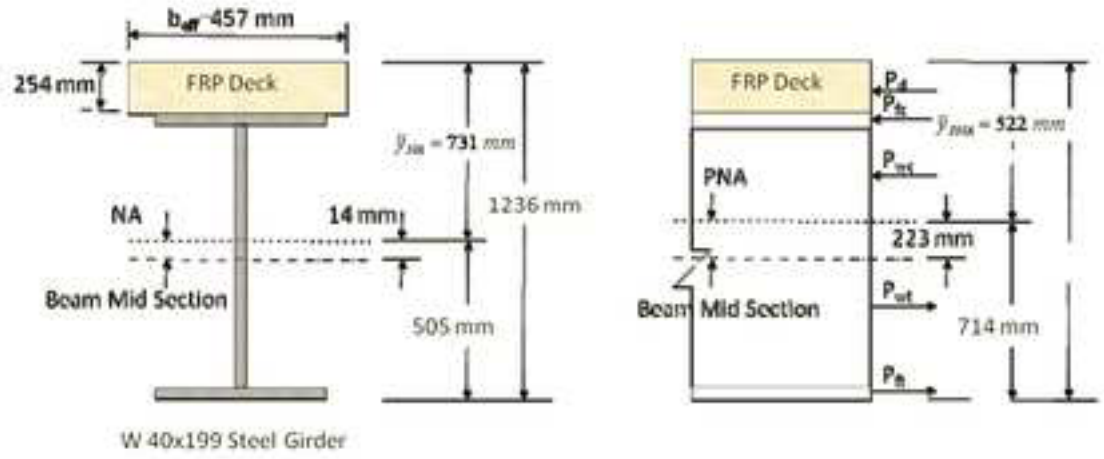

(a) Section with 25% DCA

(b) Plastic Forces for Composite Positive Moment Section

Figure 14: Partial Composite Sections